Spontaneous fission hindrance in even-odd nuclei within a cluster approach

I. S. Rogov ,[1,2] G. G. Adamian ,[1] and N. V. Antonenko[1,2]
[1] *Joint Institute for Nuclear Research, 141980 Dubna, Russia*
[2] *Tomsk Polytechnic University, 634050 Tomsk, Russia*

(Received 3 March 2022; accepted 24 March 2022; published 31 March 2022)

For even-odd isotopes of actinides and superheavy nuclei, spontaneous fission and α-decay half-lives are calculated within the dinuclear system model and compared with the existing experimental data. All these processes are considered as the evolution of a nucleus in the charge (mass) asymmetry coordinate and in the relative distance between the centers of clusters formed. The important role of the spin dependence of total potential energy in the charge asymmetry coordinate is shown and the origin of the fission hindrance in even-odd nuclei is explained.

DOI: 10.1103/PhysRevC.105.034619

I. INTRODUCTION

The stability of many heavy and superheavy nuclei, which are produced in complete fusion reactions, is determined by either α decay or spontaneous fission (SF) [1–4]. The half-life of SF increases as one goes from an even-even to an even-odd nucleus, i.e., there is the hindrance for fission of odd-mass nuclei [5]. So, there is the prominent odd-even effect in the half-life with respect to SF (about 2–7 orders of magnitude per odd particle). For example, $T_{1/2} = 1.31 \times 10^2$ y (1.5 s) for the SF of ^{257}Fm (^{259}Fm) in comparison with $T_{1/2} = 1.02 \times 10^4$ s ($\approx$0.37 ms) for the SF of ^{256}Fm (^{258}Fm). Quantitatively the reduced fission probability is expressed by a hindrance factor (HF), defined as the ratio of the experimental fission half-life and unhindered fission half-life, which is calculated as the geometrical mean of the fission half-lives of the neighboring even-even nuclei [6]. In general, the HF decreases with increasing fissility which is characterized by Z^2/A (Z and A are the charge and mass numbers of the fissioning nucleus). There is significant difference in the HF for nuclei with the same Z^2/A. Because the known SF half-lives do not exhibit any systematic behavior, it is difficult to extract the dependence of the HF on the spin of odd nucleus from the existing experimental data. The origin of the odd-even retardation has not yet been completely clarified with the fission approaches [6–9], where the quadrupole and octupole moments are assumed to be relevant collective coordinates driving the nucleus to fission. In Refs. [6–9], the fission hindrance is caused by a change in either the effective inertial parameter and/or potential barrier height and thickness, due to the change of pairing energy and specialization energy which is added to an odd particle because of spin conservation when changing the deformation along the fission path. The specialization energies of certain odd-particle orbitals is expected to give a substantial increase in the SF half-lives.

In Refs. [10,11], a new cluster approach for calculating the SF half-lives of heavy and superheavy nuclei was developed. This approach allows us to describe simultaneously the α decay, cluster radioactivity (CR), and SF. All these processes are considered as the evolution of the fissioning nucleus in the collective coordinates of charge (mass) asymmetry and relative distance between the centers of two clusters. The model of Refs. [10,11] reproduces pretty well the global isotopic trends of SF and α-decay half-lives for even-even nuclei U, Pu, Cm, Cf, Fm, No, Rf, Sg, and Hs [11]. In contrast to other existing fission models, our model gives correct absolute values of $T_{1/2}$ for SF, CR, and α decay. One of the goals of the present work is to describe the SF and α-decay half-lives for even-odd nuclei and to understand the origin of the SF hindrance for the odd-mass nuclei within the cluster approach. An intriguing question is whether the proposed cluster approach is good for even-odd nuclei as well as for even-even nuclei.

In Sec. II, we discuss our cluster model for fission. This model is employed in Sec. III to calculate the SF and α-decay half-lives of even-odd heavy nuclei with the charge numbers $Z = 96$, 100, and 104. We analyze the spin dependence of half-lives and compare the calculated half-lives with existing experimental data and the fission half-lives of the neighboring even-even nuclei. The roles of potential energy and mass parameter in the SF are studied in details. Finally, we summarize our results in Sec. IV.

II. MODEL

Fission processes are considered here within the dinuclear system (DNS) model [10,11] in which the formation of cluster with charge number $Z_L \geqslant 2$ is described as the evolution of the system in charge asymmetry coordinate

$$\eta_Z = \frac{Z_H - Z_L}{Z_H + Z_L}. \quad (1)$$

Here, Z_i (A_i), where $i = L, H$, is the charge (mass) number of the ith cluster and $Z = Z_L + Z_H$ ($A = A_L + A_H$) is the total charge (mass) number of the DNS. The $\eta_Z = 1$ corresponds to the state of mononucleus (clusterless nucleus), and $\eta_Z = 0$ is for the symmetric DNS configuration. The mass asymmetry coordinate $\eta = \frac{A_H - A_L}{A_H + A_L}$ is assumed to be strongly related to η_Z by the condition of the potential energy minimum. Indeed, at given η_Z the DNS potential energy as a function of η has a well-defined minimum. So, the spreading in η is small at each η_Z. The decay of the formed DNS is considered as a motion of the DNS in the relative distance R. Thus, the probability of finding two clusters L and H at given η_Z is proportional to the leakage of the ground-state wave function in R at this η_Z. To simplify the description of cluster decay [12–24], the process is usually divided into two independent stages: forming the cluster state or DNS, and its decay in R coordinate [24].

The probability of DNS formation (spectroscopic factor) S_L is determined by solving the stationary Schrödinger equation [10,11]

$$H\Psi_n(\eta_Z) = E_n\Psi_n(\eta_Z), \tag{2}$$

where the collective Hamiltonian

$$H = -\frac{\hbar^2}{2}\frac{\partial}{\partial\eta_Z}(B^{-1})_{\eta_Z}\frac{\partial}{\partial\eta_Z} + U(R_m, \eta_Z, \Omega) \tag{3}$$

contains the inverse inertia coefficient $(B^{-1})_{\eta_Z}$ and the potential energy U calculated at the touching distance $R = R_m$ at given η_Z. The model presented here belongs to the cluster type, because the ground state of the nucleus is assumed to have a small admixture of cluster-state components. Here, the cluster state means two touching nuclei or a DNS. The total wave function $\Psi_n(\eta_Z)$ of the nucleus is expressed by a superposition of cluster and clusterless components. Since we assume that the spin and parity of the fissioning nucleus are preserved during SF, then all cluster and clusterless components have the same spin and parity of the parent nucleus. These effects are effectively described through the inclusion of the centrifugal potential in the DNS potential energy [25]

$$U(R_m, \eta_Z, \Omega) = V(R_m, \eta_Z, \Omega) + Q_L + Q_H - Q_M, \tag{4}$$

which, as a function of charge asymmetry, is referred to as a driving potential. Here, Q_M and $Q_{L,H}$ are the experimental mass excesses [26] of the parent nucleus and the nuclei forming the DNS, respectively. The peculiarities of the structure of the DNS nuclei are taken into account through $Q_{L,H}$. The tip-tip orientation of axial symmetric deformed nuclei is taken in the calculations of driving potentials because it provides the minimum of the potential energy of the DNS considered. The nucleus-nucleus interaction potential

$$V(R, \eta_Z, \Omega) = V_C(R, \eta_Z) + V_N(R, \eta_Z) + V_r(R, \eta_Z, \Omega) \tag{5}$$

in Eq. (4) consists of the Coulomb V_C, nuclear V_N, and centrifugal V_r parts. The nuclear part V_N of the interaction potential is calculated in the double folding form, where the density-dependent nucleon-nucleon forces are folded with the nucleon densities of heavy ρ_H and light ρ_L nuclei of the DNS [10,11]. The centrifugal potential is calculated as

$$V_r = \hbar^2\Omega(\Omega + 1)/(2\Im),$$

where Ω is the spin of fissioning nucleus and

$$\Im = c_1\left(\Im_L + \Im_H + \mu R_m^2\right)$$

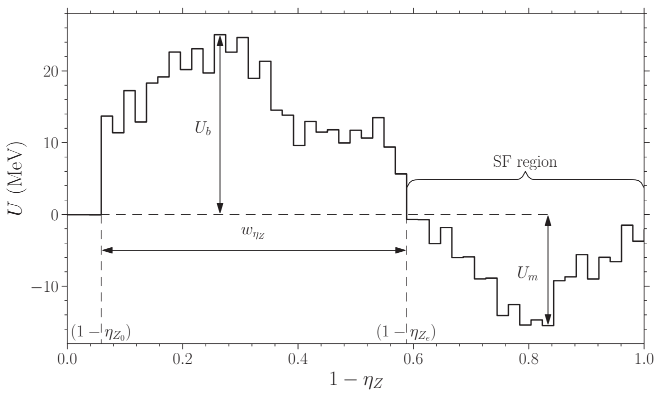

FIG. 1. Driving potential for ^{258}No. The fission barrier in η_Z is characterized by the height U_b and the width w_{η_Z}. The depth of the global potential minimum in the SF region is denoted by U_m. The tip-tip orientation of nuclei is taken in the DNS.

is the moment of inertia of the DNS, where $\Im_{L,H}$ are rigid body moments of inertia for the clusters of the DNS, $c_1 = 0.85$ for all considered fissioning nuclei [23,24,27], and $\mu = m_0 A_L A_H/(A_L + A_H)$ is the reduced mass parameter (m_0 is the nucleon mass). Note that the nucleus-nucleus potential depends on the ground-state quadrupole deformations [28] of the DNS nuclei and has a minimum at $R = R_m$ [10,11].

For the calculation of the inverse mass parameter in η_Z, we use the expression

$$(B^{-1})_{\eta_Z} = \frac{1}{2m_0}\frac{A_{\text{neck}}}{2\sqrt{2\pi}b^2A^2}, \tag{6}$$

which was derived in Ref. [29]. Here, b characterizes the DNS neck size and

$$A_{\text{neck}} = \int [\rho_L(\mathbf{r}) + \rho_H(\mathbf{R_m} - \mathbf{r})] \exp\left(-\frac{z^2}{b^2}\right) d\mathbf{r}$$

is the number of nucleons in the neck region between two nuclei. In the present calculations, we set the neck parameter $b = 0.479–0.019\eta_Z$ fm, which corresponds to about three to five nucleons in the neck region. Slightly larger b for the symmetric DNS reflects a larger number of nucleons in the neck region between two heavy nuclei.

The driving potential for the fissioning nucleus ^{258}No is shown in Fig. 1. The values of U and $(B^{-1})_{\eta_Z}$ are extended to the segments of the width $2\Delta = 2/Z$ so that the points η_Z are placed in the middle of the corresponding segments. The only exception is the mononucleus, for which we set $\eta_Z \in [1, 1 - 4\Delta)$ and the α-particle DNS with $\eta_Z \in [1 - 4\Delta, 1 - 5\Delta)$. Indeed, the SF mainly occurs from the DNS configurations corresponding to the minima of the driving potential with energies smaller than the ground-state energy [10,11], i.e., at about $1 - \eta_Z > 0.6$. To undergo SF and be in the energy-resolved region with the global potential minimum of the depth U_m at $\eta_Z \approx 0.2$, the fissioning nucleus should pass through a barrier of height U_b and width w_{η_Z} (Fig. 1). The values $1 - \eta_{Z_0}$ and $1 - \eta_{Z_e}$ are the entrance and exit turning points, respectively. Note that SF events occurs also from the

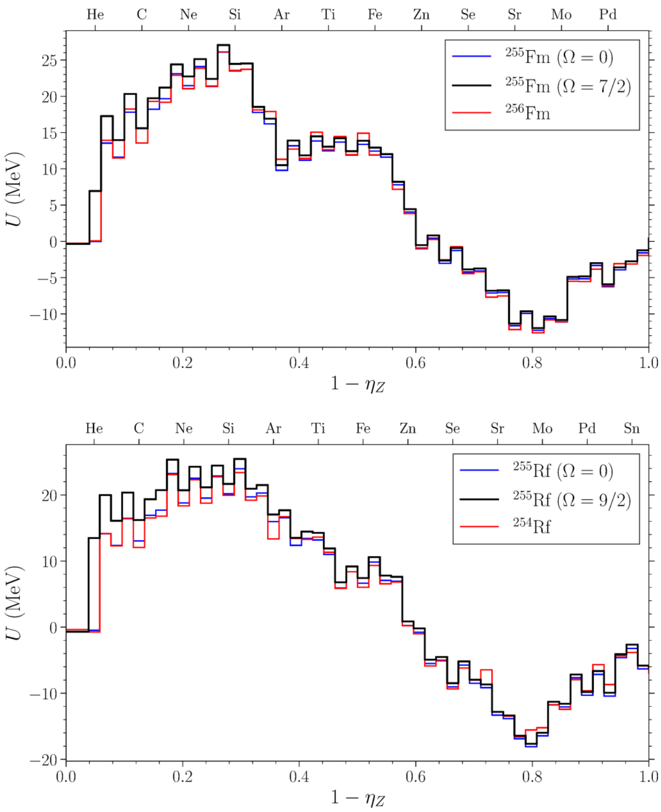

FIG. 2. Calculated driving potentials U with nonzero and zero Ω as the step functions of $1 - \eta_Z$ for ^{255}Fm and ^{255}Rf. The light nuclei of the DNS are indicated on the upper horizontal axes.

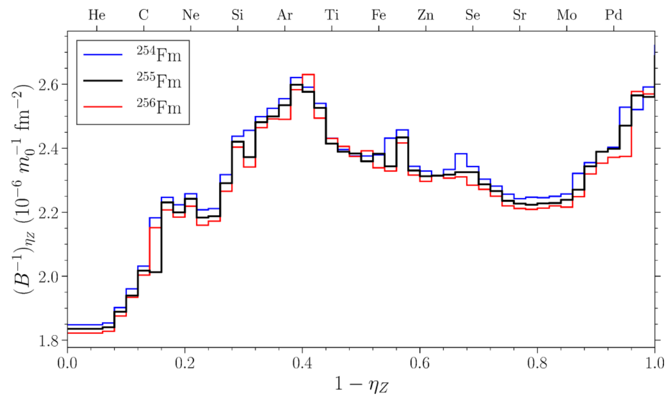

FIG. 3. Calculated inverse mass parameters $(B^{-1})_{\eta_Z}$ for ^{254,255,256}Rf as the step functions of $1 - \eta_Z$. The light nuclei of the DNS are indicated on the upper horizontal axes.

sub-barrier region but their contributions are negligible compared to the contributions from the energy-resolved region.

The preformation probability S_L of the DNS with certain charge number Z_L of light cluster is defined as

$$S_L = \int_{\eta_Z(Z_L)-\Delta}^{\eta_Z(Z_L)+\Delta} |\Psi(\eta_Z)|^2 d\eta_Z. \tag{7}$$

For the α decay and cluster radioactivity in the potential barrier region at about $1 - \eta_Z \leqslant 0.6$ (Fig. 1), the half-life is calculated as

$$T_{1/2} = \frac{\hbar \ln 2}{\Gamma_L} = \frac{\pi \ln 2}{\omega_0 S_L P_L}, \tag{8}$$

where Γ_L is the decay width and

$$P_L = \left(1 + \exp\left[\frac{2}{\hbar}\int_{R_m}^{R_e} \sqrt{2\mu[V(R, \eta_Z(Z_L)) - Q]}dR\right]\right)^{-1}$$

is the penetration probability through the Coulomb barrier calculated in the WKB approach (R_e is the exit point from the potential V and Q is the decay energy). The value of frequency ω_0 of zero-point vibration in the η_Z coordinate near the mononucleus state ($\eta_Z \approx 1$) is equal to the distance between the ground and the first excited state of DNS vibrating in η_Z.

In the case of SF, all DNS configurations in the SF region contribute because their decay probabilities P_L in R coordinate are equal to 1. Therefore, the SF half-life is calculated as

$$T_{1/2} = \frac{\pi \ln 2}{\omega_0 S_{\mathrm{SF}}}, \tag{9}$$

where

$$S_{\mathrm{SF}} = \int_0^{\eta_{Z_e}} |\Psi(\eta_Z)|^2 d\eta_Z \tag{10}$$

and η_{Z_e} is the exit turning point (see Fig. 1).

TABLE I. Spectroscopic factors S_α and S_α^*, energies of the first excited state $\hbar\omega_0$ and $\hbar\omega_0^*$, SF half-lives $T_{1/2}$ and $T_{1/2}^*$ for even-odd isotopes, and the geometrical means $T_{1/2}^{est}$ of the experimental fission half-lives of the neighboring even-even nuclei [30]. The quantities S_α^*, $\hbar\omega_0^*$, and $T_{1/2}^*$ are calculated at $\Omega = 0$.

	Ω	S_α	S_α^*	$\hbar\omega_0$ (MeV)	$\hbar\omega_0^*$ (MeV)	$T_{1/2}$ (s)	$T_{1/2}^*$ (s)	$T_{1/2}^{\mathrm{est}}$ (s)
^{243}Cm	5/2	0.0526	0.0707	1.20	1.19	2.57×10^{18}	1.02×10^{14}	2.75×10^{14}
^{245}Cm	7/2	0.0428	0.0947	1.17	1.10	1.65×10^{20}	7.34×10^{14}	4.35×10^{14}
^{243}Fm	7/2	0.0712	0.0904	1.80	1.63	3.51	3.14×10^{-4}	2.08×10^{-4}
^{255}Fm	7/2	0.0527	0.0816	1.35	1.26	3.01×10^{11}	1.62×10^{6}	1.16×10^{6}
^{257}Fm	9/2	0.0481	0.0888	1.38	1.56	4.13×10^{9}	1.19	4.02
^{253}Rf	7/2	0.0888	0.0947	1.00	1.01	7.76×10^{-1}	1.23×10^{-4}	–
^{255}Rf	9/2	0.0691	0.0930	1.27	1.48	2.00	2.95×10^{-3}	4.14×10^{-4}
^{257}Rf	1/2	0.0893	0.0918	1.36	1.18	1.11×10^{1}	3.99×10^{-2}	1.05×10^{-2}

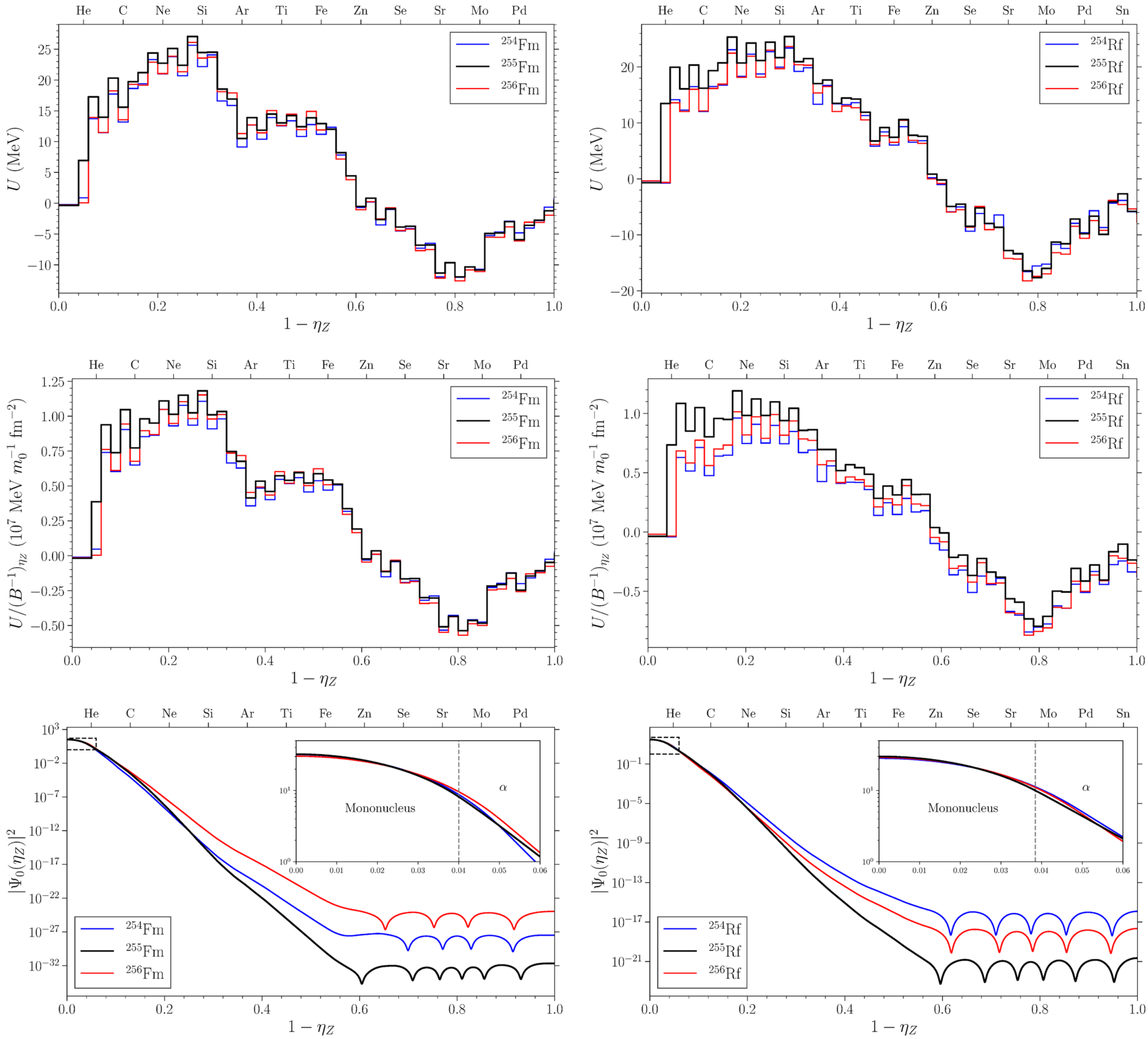

FIG. 4. Calculated driving potentials U, ratios $U/(B^{-1})_{\eta_Z}$, and the squares of the module of the ground-state wave functions $|\Psi_0|^2$ for ^{255}Fm ($\Omega = 7/2$) and ^{255}Rf ($\Omega = 9/2$) as the functions of $1-\eta_Z$. The light nuclei of the DNS are indicated on the upper horizontal axes.

III. CALCULATED RESULTS

As shown in Fig. 2, the driving potentials U have the global maxima and minima. The energy of the initial fissioning nucleus (mononucleus) at $\eta_Z = 1$ is larger than the potential energies in the minimum at $\eta_Z < 0.4$ corresponding to the energy-resolved region for fission. Thus, the energy-resolved DNS configurations appear in the SF.

In the case of isotopes ^{254,255,256}Fm and ^{254,255,256}Rf, on the average

$$U(^{255}\mathrm{Fm}) > U(^{254,256}\mathrm{Fm})$$

and

$$U(^{255}\mathrm{Rf}) > U(^{254,256}\mathrm{Rf})$$

in the region of fission barrier (Fig. 2). This leads to the enhancement of SF $T_{1/2}$ for ^{255}Fm and ^{255}Rf with respect to corresponding neighboring even-even nuclei. Let us discuss the reason of an effective increase of the fission barrier for even-odd nuclei.

For the fissioning even-odd nuclei with nonzero spin, the centrifugal potential strongly affects the shape of the driving potential, especially in the region of asymmetric DNS. As seen in Fig. 2 for ^{255}Rf, the potential energy at spin $\Omega = 9/2$ becomes higher, than the potential energy at $\Omega = 0$, especially for the α-particle configuration. The difference between the driving potentials at $\Omega = 0$ and $\Omega = 9/2$ is almost insignificant in the region $(1-\eta_Z) > 0.5$. The same dependence on Ω is seen for ^{255}Fm in Fig. 2. Again the absolute value of the potential energy in the asymmetric region increases with the value of spin Ω. The driving potential for ^{255}Rf (^{255}Fm) at $\Omega = 0$ is relatively close to that for ^{254}Rf (^{254}Fm) (Fig. 2). Indeed, in Table I, the calculated half-life $T_{1/2}(\Omega = 0)$ for ^{255}Rf (^{255}Fm) at $\Omega = 0$ and geometrical mean $T_{1/2}^{est} = [T_{1/2}^{\exp}(^{254}\mathrm{Rf})T_{1/2}^{\exp}(^{256}\mathrm{Rf})]^{1/2}$ ($T_{1/2}^{est} = [T_{1/2}^{\exp}(^{254}\mathrm{Fm})T_{1/2}^{\exp}(^{256}\mathrm{Fm})]^{1/2}$) of the experimental fission half-lives of the neighboring even-even nuclei differ only 7.1 (1.4) times. For other nuclei ^{243,245}Cm, ^{243,257}Fm, and ^{253,257}Rf in Table I, $T_{1/2}(\Omega = 0)$ and $T_{1/2}^{est}$ differ less than 4 times. So, one can conclude that the rotational energy in the driving potential is mainly responsible for the fission hindrance in even-odd nuclei. The spin dependence of the driving potential leads to the reduction of the formation probabilities of the almost symmetric binary cluster configurations in the energy-resolved region at about $1 - \eta_Z > 0.6$.

Since the mass parameter for an odd nucleus is close in magnitude to the mass parameters of neighboring even-even nuclei, the role of the mass parameter in the hindrance of fission is much weaker than the role of potential energy. As an example, we show in Fig. 3 the mass parameters for the nuclei ^{254,255,256}Fm. Thus, the potential energy, or rather the centrifugal potential, plays a major role in the hindrance of fission.

The potential barrier penetrability in the charge asymmetry coordinate depends on the ratio $U/(B^{-1})_{\eta_Z}$ of the potential energy and the inverse mass parameter [11]. For the fissioning nuclei ^{254,255,256}Fm and ^{254,255,256}Rf, the ratios $U/(B^{-1})_{\eta_Z}$ and the squares of the module of the ground-state wave functions $|\Psi_0|^2$ are presented in Fig. 4 together with the driving potentials U as functions of $1 - \eta_Z$. As clearly seen, on average

$$\frac{U}{(B^{-1})_{\eta_Z}}(^{255}\mathrm{Fm}) > \frac{U}{(B^{-1})_{\eta_Z}}(^{254,256}\mathrm{Fm})$$

and

$$\frac{U}{(B^{-1})_{\eta_Z}}(^{255}\mathrm{Rf}) > \frac{U}{(B^{-1})_{\eta_Z}}(^{254,256}\mathrm{Rf})$$

in the potential barrier region, and, correspondingly,

$$|\Psi_0|^2(^{255}\mathrm{Fm}) < |\Psi_0|^2(^{254,256}\mathrm{Fm})$$

and

$$|\Psi_0|^2(^{255}\mathrm{Rf}) < |\Psi_0|^2(^{254,256}\mathrm{Rf})$$

in the energy-resolved region ($1 - \eta_Z > 0.6$). As a result, for SF

$$T_{1/2}(^{255}\mathrm{Fm}) < T_{1/2}(^{254,256}\mathrm{Fm})$$

and

$$T_{1/2}(^{255}\mathrm{Rf}) < T_{1/2}(^{254,256}\mathrm{Rf}).$$

The calculated half-lives of even-odd and even-even nuclei are in a good agreement with the available experimental data for α decay and SF (Fig. 5). For the SF (α decay) of ^{235}U, ^{239}Pu, and ^{241}Pu, $T_{1/2} = 1.65 \times 10^{26}$, 5.39×10^{23}, and 3.04×10^{24} s ($T_{1/2} = 6.49 \times 10^{16}$, 2.73×10^{11}, and 2.60×10^{13} s), while the experimental half-lives are $T_{1/2} = 3.19 \times 10^{26}$, 2.54×10^{23}, and $\approx 1.89 \times 10^{24}$ s ($T_{1/2} = 2.23 \times 10^{16}$, 7.61×10^{11}, and 4.52×10^{13} s), respectively. For the fissioning nuclei

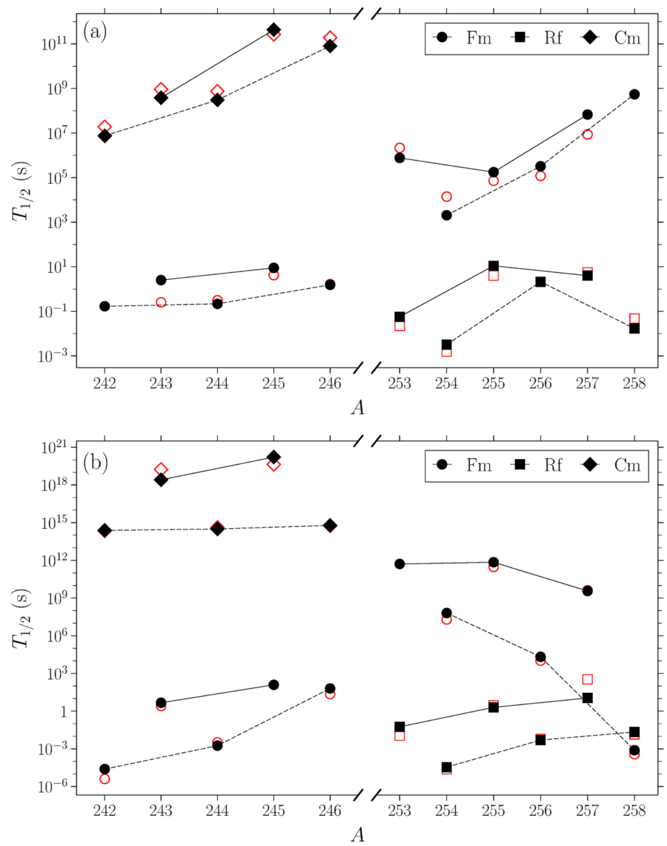

FIG. 5. Calculated and experimental α-decay (a) and spontaneous fission (b) half-lives for Cm, Fm, Rf isotopes. Black solid and red open symbols represent theoretical results and experimental data [30], respectively. The even-odd (even-even) isotopes are connected with solid (dashed) lines to guide eyes. For some nuclei, the theoretical and experimental half-lives almost coincide, and the red open symbol is not clearly visible.

^{235}U, ^{239}Pu, and ^{241}Pu, the measured HF are, respectively, 518, 1.1×10^5, and $\approx 6.7 \times 10^5$ [6]. Note that our model describes well the SF half-lives of even-even actinides [11]. Using the calculated $\Omega = 1/2$ from Ref. [31], we predict $T_{1/2} = 124$ s for the SF of ^{245}Fm. As seen in Fig. 5, the α-decay and SF half-lives of even-odd isotopes are larger than expected geometrically mean half-lives of the neighboring even-even nuclei. This means that the odd-even effects of α-decay and SF half-lives are correctly included in the model. For the SF, the the rotational term of the driving potential is mainly responsible for this effect. It shifts the ground-state wave function towards the mononucleus configuration and strongly reduces the probabilities of the DNS formation in the SF region with $1 - \eta_Z > 0.6$ (Fig. 4). For the α decay, the penetration probability P_L plays important role. The centrifugal potential increases the height of Coulomb barrier and, correspondingly, decreases P_L and $T_{1/2}$. For even-odd and neighboring even-even nuclei, the probabilities of α-particle formation do not differ much from each other (Fig. 4).

For even-odd nuclei, the SF half-lives can be presented as follows:

$$T_{1/2} = F T_{1/2}(\Omega = 0), \tag{11}$$

TABLE II. Spontaneous fission half-lives $T_{1/2}^{\rm fit}$ calculated with Eq. (11) and parameter $c = 0.086$ MeV$^{-1/2}$s^{-1} in comparison with the experimental data [30].

Nucleus	Ω	$T_{1/2}(\Omega = 0)$ (s)	$(B^{-1})_{\eta_{Z_\alpha}}$ (MeV s^{-2})	F	$T_{1/2}^{\rm fit}$ (s)	$T_{1/2}^{\rm exp}$ (s)
^{243}Cm	5/2	1.02×10^{14}	8.52×10^{-3}	3.47×10^{3}	3.54×10^{17}	2.57×10^{18}
^{243}Fm	7/2	3.14×10^{-4}	2.08×10^{-2}	1.20×10^{4}	3.77	4.64
^{245}Cm	7/2	7.34×10^{14}	8.40×10^{-3}	2.63×10^{6}	1.93×10^{21}	1.65×10^{20}
^{253}Rf	1/2	2.21×10^{-5}	2.25×10^{-2}	1.54	3.40×10^{-5}	5.64×10^{-2}
^{255}Fm	7/2	1.62×10^{6}	9.98×10^{-3}	7.72×10^{5}	1.25×10^{12}	7.04×10^{11}
^{255}Rf	9/2	2.95×10^{-3}	4.22×10^{-2}	3.17×10^{4}	9.38×10^{1}	2.00
^{257}Fm	9/2	1.19	1.18×10^{-2}	3.33×10^{8}	3.96×10^{8}	3.64×10^{9}
^{257}Rf	1/2	2.02×10^{-2}	1.94×10^{-2}	1.59	3.21×10^{-2}	1.15×10^{1}

where for the HF we suggest the parametrization

$$F = \exp\left[\frac{c\Omega(\Omega+1)}{\sqrt{(B^{-1})_{\eta_{Z_\alpha}}}}\right],$$

which includes the mass parameter $(B^{-1})_{\eta_{Z_\alpha}}$ of the DNS with α particle. This mass parameter is calculated with Eq. (6). The parameter $c = 0.086$ MeV$^{-1/2}$s^{-1} is suitable for most nuclei with different Ω, except for $\Omega = 1/2$. In the case of $\Omega = 1/2$, the rotational part effect is not limited only to the α-particle state and the parameter $c = 1.14$ MeV$^{-1/2}$s^{-1} better corresponds to experimental data. This allows us to conclude that the contribution of α-particle configuration to SF hindrance rapidly increases with $\Omega > 1/2$. As seen in Table II, the expression (11) with corresponding c describes the SF half-lives well. Based on our calculations, the HF for SF of most even-odd nuclei can be roughly estimated as $F \approx \exp[0.75\Omega(\Omega+1)]$.

IV. SUMMARY

An advantage of the cluster approach is the simultaneous description of α decay and SF from the ground state of both even-even and even-odd nuclei with the same set of parameters. The main assumption of the model is that charge asymmetry as the corresponding collective variable is responsible for these processes. The absolute values of SF and α-decay half-lives of even-even and even-odd nuclei in the ground state are in a good agreement with the existing experimental data. As shown for the fissioning even-odd nuclei, the centrifugal potential is strongly affects the shape of the driving potential in the region of asymmetric DNS (especially the DNS with α particle) increasing the potential energy, for example, the height of the potential barrier, and finally creating the fission hindrance. So, within the cluster approach the origin of the SF hindrance is related with the spin dependence of the formation probabilities of the binary cluster configurations which are attributed to the SF. As found, the effect of the inertia parameter on the fission hindrance is weaker compared to the effect of potential energy, and the HF is the degree of spin-hindered fission. In the future this finding can be used to describe the SF from ground and isomeric states of odd-even and odd-odd nuclei.

ACKNOWLEDGMENT

This work was partly supported by the Ministry of Science and Higher Education of the Russian Federation (Contract No. 075-10-2020-117).

[1] Yu. Ts. Oganessian, J. Phys. G: Nucl. Part. Phys. **34**, R165 (2007).

[2] Yu. Ts. Oganessian and V. K. Utyonkov, Nucl. Phys. A **944**, 62 (2015); Rep. Prog. Phys. **78**, 036301 (2015).

[3] S. Hofmann and G. Münzenberg, Rev. Mod. Phys. **72**, 733 (2000).

[4] S. Hofmann *et al.*, Eur. Phys. J. A **52**, 116 (2016); **52**, 180 (2016).

[5] D. C. Hoffman and M. R. Lane, Radiochimca Acta **70/71**, 135 (1995).

[6] F. P. Heßberger, Eur. Phys. J. A **53**, 75 (2017).

[7] J. Randrup, C. F. Tsang, P. Möller, S. G. Nilsson, and S. E. Larsson, Nucl. Phys. A **217**, 221 (1973).

[8] Z. Łojewski and A. Baran, Z. Phys. A **322**, 695 (1985).

[9] W. Brodzinski, M. Kowal, J. Skalski, and P. Jachimowicz, Acta Phys. Pol. B **49**, 621 (2018).

[10] I. S. Rogov, G. G. Adamian, and N. V. Antonenko, Phys. Rev. C **100**, 024606 (2019).

[11] I. S. Rogov, G. G. Adamian, and N. V. Antonenko, Phys. Rev. C **104**, 034618 (2021).

[12] R. K. Gupta, S. Singh, R. K. Puri, and W. Scheid, Phys. Rev. C **47**, 561 (1993).

[13] Yu. M. Tchuvil'sky, *Cluster Radioactivity* (Moscow State University, Moscow, 1997).

[14] W. Greiner, M. Ivascu, D. N. Poenaru, and A. Sandulescu, in *Treatise on Heavy Ion Science*, edited by D. A. Bromley (Plenum, New York, 1989), Vol. 8, p. 641.

[15] Yu. S. Zamyatnin *et al.*, Sov. J. Part. Nucl. **21**, 231 (1990).

[16] S. G. Kadmensky, S. D. Kurgalin, and Yu. M. Tchuvil'sky, Phys. Part. Nucl. **38**, 699 (2007).

[17] D. N. Poenaru, *Nuclear Decay Modes* (IOP Publishing, Bristol, 1996).

[18] K. Varga, R. G. Lovas, and R. J. Liotta, Phys. Rev. Lett. **69**, 37 (1992).
[19] N. Itagaki, J. Cseh, and M. Ploszajczak, Phys. Rev. C **83**, 014302 (2011).
[20] J. Cseh, A. Algora, J. Darai, and P. O. Hess, Phys. Rev. C **70**, 034311 (2004); A. Algora, J. Cseh, J. Darai, and P. O. Hess, Phys. Lett. B **639**, 451 (2006).
[21] W. Sciani, Y. Otani, A. Lépine-Szily, E. A. Benjamim, L. C. Chamon, R. L. Filho, J. Darai, and J. Cseh, Phys. Rev. C **80**, 034319 (2009); J. Cseh, J. Darai, W. Sciani, Y. Otani, A. Lépine-Szily, E. A. Benjamim, L. C. Chamon, and R. L. Filho, *ibid.* **80**, 034320 (2009).
[22] D. Lebhertz, S. Courtin, F. Haas, D. G. Jenkins, C. Simenel, M. D. Salsac, D. A. Hutcheon, C. Beck, J. Cseh, J. Darai, C. Davis, R. G. Glover, A. Goasduff, P. E. Kent, G. Levai, P. L. Marley, A. Michalon, J. E. Pearson, M. Rousseau, N. Rowley *et al.*, Phys. Rev. C **85**, 034333 (2012).
[23] S. N. Kuklin, G. G. Adamian, and N. V. Antonenko, Yad. Fiz. **68**, 1501 (2005) [Phys. At. Nucl. **68**, 1443 (2005)]; Phys. Rev. C **71**, 014301 (2005); Yad. Fiz. **71**, 1788 (2008) [Phys. At. Nucl. **71**, 1756 (2008)]; S. N. Kuklin, T. M. Shneidman, G. G. Adamian, and N. V. Antonenko, Eur. Phys. J. A **48**, 112 (2012).
[24] G. G. Adamian, N. V. Antonenko, and W. Scheid, in *Lecture Notes in Physics* 848, *Clusters in Nuclei*, Vol. 2, edited by C. Beck (Springer-Verlag, Berlin, 2012), p. 165.
[25] G. G. Adamian *et al.*, Int. J. Mod. Phys. E **05**, 191 (1996).
[26] J. K. Tuli, *Nuclear Wallet Cards* (BNL, New York, 2000).
[27] T. M. Shneidman, G. G. Adamian, N. V. Antonenko, R. V. Jolos, and W. Scheid, Phys. Lett. B **526**, 322 (2002); Phys. Rev. C **67**, 014313 (2003); **70**, 064318 (2004).
[28] S. Raman *et al.*, At. Data Nucl. Data Tables **78**, 1 (2001); P. Möller and J. J. Nix, *ibid.* **39**, 213 (1988).
[29] G. G. Adamian, N. V. Antonenko, and R. V. Jolos, Nucl. Phys. A **584**, 205 (1995).
[30] http://www.nndc.bnl.gov/nndc/ensdf/.
[31] G. G. Adamian, N. V. Antonenko, S. N. Kuklin, B. N. Lu, L. A. Malov, and S.-G. Zhou, Phys. Rev. C **84**, 024324 (2011).